Journal of Energy Challenges and Mechanics
http://www.nscj.co.uk/JECM/
ISSN 2056-9386
Volume 1 (2014) issue 2, article 3

Operation of intelligent wind power unit

智能風力発電机器的工作

Ahmed Mohamed Galal[1], Toshiaki Kanemoto[2*], Kazumasa Makita[3] and Yusuke Taneo[3]

[1]*Faculty of Engineering, Mansoura University, Mansoura, Egypt*
[2]*Faculty of Engineering, Kyushu Institute of Technology, Kitakyushu 804-8550, Japan*
[3]*Graduate School of Engineering, Kyushu Institute of Technology, Kitakyushu 804-8550, Japan*

kanemoto@mech.kyutech.ac.jp

Accepted for publication on 22th July 2014

Abstract – **The Intelligent Wind Power Unit is composed of a large-sized front wind rotor, a small-sized rear wind rotor and a peculiar generator with double rotational armatures without the traditional stator. The superior operation of the tandem wind rotors has been verified and the desirable profile of the rotors has been presented in previous papers. In this paper, the blade setting angle is adjusted, not only to get a maximum efficiency at lower wind velocity but also to keep the output constant at the rated operation in the laboratory experiments. The model unit with the double rotational armature type doubly-fed induction generator is also provided for the natural wind circumstance, and the output performance is adjusted well with the exciting voltage and the frequency of the secondary circuit in the generator.**

Keywords – **Wind turbine, Tandem wind rotors, Generator.**

I. INTRODUCTION

Wind power is one of significantly promising resources for sustainable/renewable energies that may play a very important role in electric power generation at the 21st century. Wind turbines have been developed/improved to increase the output, and have been positively/effectively provided for the grid system. The authors have also invented a superior wind power unit, "Intelligent Wind Power Unit", as shown in Fig.1 [1][2]. The unit is composed of a large-sized front wind rotor, a small-sized rear wind rotor and a peculiar generator with double rotational armatures without the traditional stator. The front and the rear wind rotors drive the inner and the outer rotational armatures, respectively. Rotational speeds and directions of both wind rotors/armatures are automatically adjusted pretty well in response to wind circumstances.

The idea of tandem wind rotors has been proposed before [3]-[9], but not only the profiles but also the operations of the experiments on tandem wind rotors quite differ from those surveyed above. That is, the rotational directions and speeds of both wind rotors/armatures are automatically adjusted in response to the wind velocity. Both wind rotors start to rotate at low wind velocity, namely the cut-in wind velocity, but the rear wind rotor counter-rotates against the front wind rotor. The rear wind rotor reaches the maximum rotational speed at the rated wind velocity. With more increase of the wind velocity, the rotational speed of the rear wind rotor decreases gradually, stops and then begins to rotate at the same direction of the front wind rotor, so as to coincide with the larger rotational torque of the front wind rotor.

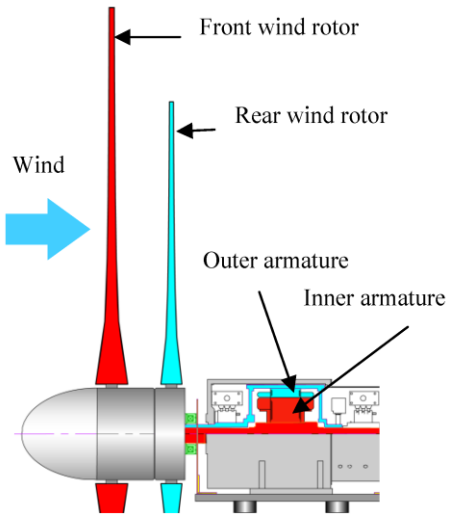

Fig. 1 Profile of Intelligent Wind Power Unit

Such superior operations of the tandem wind rotors have been verified experimentally and the desirable profiles of the wind rotors have been proposed [10]-[12]. Continuously, in this paper, the blade setting angle is adjusted, not only to get a maximum efficiency at lower wind velocity but also to keep

the output constant at the rated operation in the laboratory experiments. The model unit equipped with the double rotational armature type doubly-fed induction generator is also provided for the natural wind circumstance.

II. Adjustment of Blade Setting Angle Experiments in a Wind Tunnel

The model tandem wind rotors were set, perpendicularly to the wind direction, at the outlet of the wind tunnel with nozzle diameter of 800 mm. The front and the rear wind rotors connected directly and respectively to the isolated motors controlled by the inverter with the regenerative braking system, in place of the peculiar generator. The diameter of the front wind rotor is d_F = 500 mm with three blades, and the rear wind rotor is d_R = 420 mm with five blades. The axial distance between the twist center of the front and the rear blade is l= 40 mm. The diameter ration and the number of blades have been optimized at the laboratory researches [11] [13].

In the experiments, the rotational torques of the front and the rear wind rotors were counter-balanced by the rotational speed control in place of the double rotational armatures. The output is evaluated without the mechanical losses of bearings and pulley systems. The Reynolds number estimated with the relative velocity component and the chord length at the blade tip is Re = 5.8 x 10^4 - 1.8 x 10^5, which may be less than Re for prototypes but is in close to the turbulent flow because the higher fluctuation V' with RMS(V')/V = 3.6 % (V'_{max}/V = 11 %, V: the wind velocity) at the nozzle outlet promotes the transition from the laminar to the turbulent flows on the blade surfaces.

Optimization of Front Blade Profile

Previous research has suggested that the front wind rotor, at the smaller radius, had better not to absorb the wind energy but better to give away enough wind energy to the rear wind rotor [12]. That is, the front wind rotor never generates the swirling velocity component at the smaller radius while the coming flow is in axial direction.

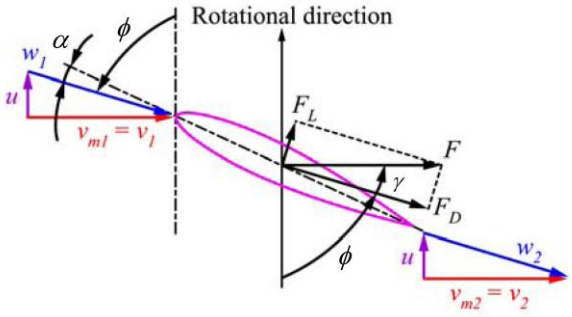

Fig. 2 Flow conditionround the front wind rotor at the smaller radius

Figure 2 shows the velocity triangles around the front blade at the smaller radius, where v, u, w and v_m are the absolute, the rotational, the relative, and the axial velocity components (subscripts 1 and 2 mean the inlet and the outlet). The resultant force F must be in the axial direction and has no tangential component. Equation (1) gives the lift-drag ratio ε and Equation (2) gives the relative flow angle ϕ, while Equation (3) gives the angle γ between the drag force F_D and F.

$$\varepsilon = F_L / F_D = u / v_{m1} = r\omega / v_{m1} \quad (1)$$

$$\phi = \tan^{-1}(v_{m1} / r\omega) = \tan^{-1}(F_D / F_L) \quad (2)$$

$$\gamma = \tan^{-1}(F_L / F_D) = \tan^{-1}\varepsilon \quad (3)$$

The blade must twist in the radial direction so as to satisfy $\phi + \gamma$ = 90 degrees while F is in the axial direction, and to make F_D , which decelerates the axial velocity, as small as possible.

Front Blade H shown in Fig. 3(a) was designed on the basis of the above advanced technology at the tip speed ratio λ_F = (blade tip speed)/V = 4.5 and formed with NACA0015 symmetric airfoil [15] at the smaller radius (0.2 < R < 0.46, R: the dimensionless radius divided by d_F/2). The blade at the larger radius (0.54 < R) has MEL002 airfoil [14] with the desirable angle of attack to get fruitful wind energy. Rear Blade G shown in Fig. 3(b) was formed tentatively with MEL002 airfoil [14] and was twisted to have the desirable angle of attack, taking account of the flow discharged from the front wind rotor. The tandem wind rotors designed just above (TWR HG) takes the maximum output coefficient of C_P = $P/(\rho AV^3/2)$ = 0.35 at the relative tip speed ratio λ_T = 6.3, where P is the output and A is the swept area of the front wind rotor.

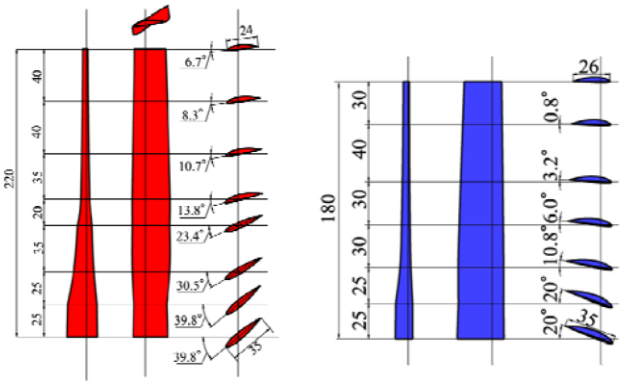

(a)Front Blade H (b)Rear Blade G

Fig. 3 Blade profiles for the tandem wind rotors

Performance Against Wind Velocity

It may be possible to adjust the blade setting angle of the rear wind rotor, β_R, because the rotor is connected to the outer shaft as shown in Fig. 1, which can be easily equipped with a pitch control mechanism of the blade. Figure 4 shows the performance against the wind velocity, while β_R is adjusted to get a maximum efficiency under V = 10 m/s and get a constant output P_T at the rated operation in keeping the blade setting angle of the front wind rotor β_F = 5 degrees, where the angles are measured between the blade chord and the rotational directions at the blade tip. It is necessary to adjust the blade setting angle β_R for aerodynamically keeping the output constant at the rated operation. The relative rotational speed N_T = N_F - N_R decreases at the wind velocity V faster than 10 m/s,

as the increase of V accompanies the increase of the rotational torque.

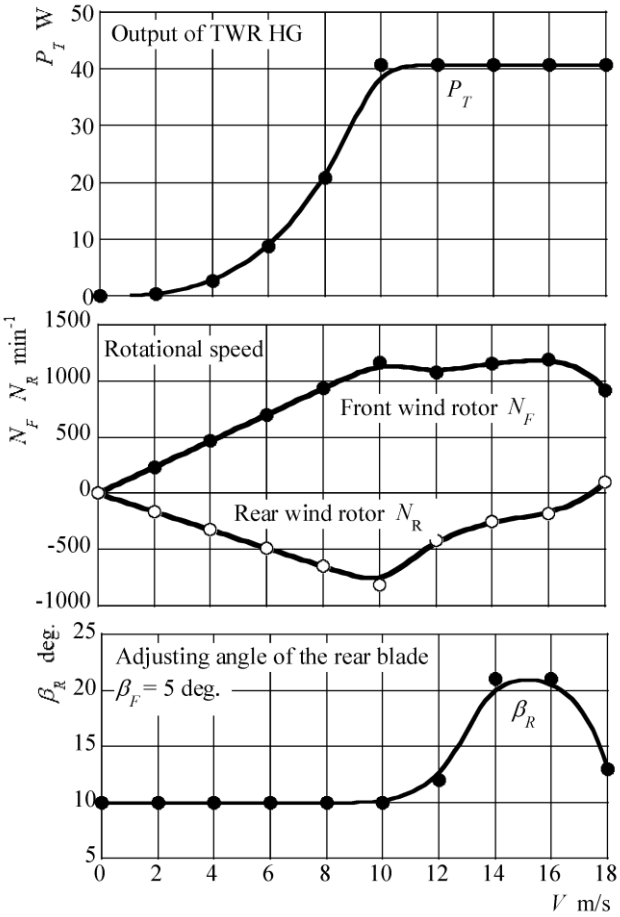

Fig. 4 Performance of the model unit in the wind tunnel

III. Operation in Natural Wind Preparation of the Model Unit

The upwind type unit shown in Fig. 5 was prepared for the field tests. The front wind rotor has the diameter of d_F = 2000 mm and is composed of three blades. The rear wind rotor has the diameter of d_R = 1640 mm and is composed of five blades. The axial distance between both wind rotors is l = 160 mm. These dimensions have also been optimized in previous papers [11][13]. The blade profiles of the front and the rear wind rotors are shown in Fig. 6, where these are designed on the basis of the advanced technology described above. The aerofoil sections of the blades are almost similar to those in Fig. 3, but the front blade at the smaller radius is formed with cambered aerofoil without load.

Fig. 5 Model unit

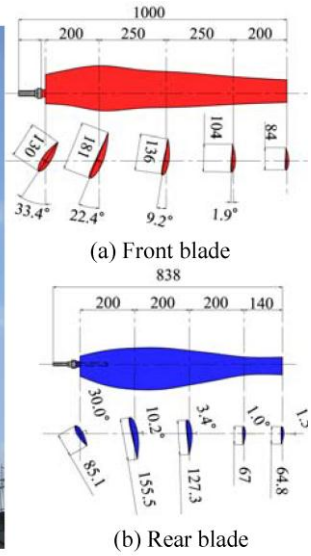

Fig. 6 Blade profiles

The above tandem wind rotors counter-drive the inner and the outer armatures in the doubly-fed induction generator (3-phase, 8-poles, [16]). The generator is composed of the primary circuit in the outer armature which induces the active power P_1, corresponding P_T in Fig. 3, and the secondary circuit in the inner armature which consume the reactive power for rotating the excited magnetic field. The rated output of the generator is 1.2 kW with the induced frequency f_1 = 60 Hz and the induced voltage E_1 = 200 V from the primary circuit while the relative rotational speed between the double rotational armatures is N_T = 900 min^{-1}. The induced frequency f_1 is determined with the rotational speed N_T and the exciting frequency f_2 at the secondary circuit. The exciting voltage E_2 at the secondary circuit, however, must be adjusted carefully in response to N_T, namely the wind velocity V, to keep E_1 and f_1 constant in the turbulent flow.

The model unit prepared above was installed on the tower of 2.4 m height which is set at the top roof of the building of 8 m height in the campus as shown in Fig. 5. The wind velocity was measured by the supersonic anemometer which is in front of the front wind rotor at the shaft centre and can detect the three dimensional flow directions.

Wind Circumstances at the Test Site

The test site has tall trees at the northern side and buildings at the southern side. These obstacles affect doubtlessly the wind circumstances from the north and the south. The wind rotor when facing the wind from the west side has comparatively better circumstance but may be poor for the power generation. Most of the time, the wind velocity is slower than 11 m/s while 3 m/s gives the highest apparent ratio with about 70 % appearance in 2~5 m/s, which may represent the wind circumstances at an urban area in Japan.

Performance Control at Natural Wind

Figure 7 shows a small example for the rotational speed of the front and the rear wind rotors, N_F, N_R, the active output P_1,

the induced voltage E_1, and the induced electrical current I_1 from the primary circuit against the wind velocity V, while the bulb load P_{bulb} = 600 W, namely the electrical resistance as the power consumption, and the exciting voltage E_2 = 60 V, the exciting frequency f_2 = 50 Hz at the secondary circuit. The experimental date accumulated during the test was averaged each one minute and the white circles in the figure represent the performances averaged each 0.5 m/s band [17]. The output P_1 and the rotational speeds N_F, N_R are widely distributed even at the same wind velocity, because the small-sized wind rotors are sensitive to the turbulent/velocity fluctuation and/or wind direction in the natural wind. The front and the rear wind rotor start counter- rotating at slow wind speed and these speeds increase with the increase of the wind velocity. The induced voltage E_1 is in proportion to the relative rotational speed $N_T = N_F - N_R$, and P_1 = square-root(3)E_1I_1, where I_1 is the induced electrical current.

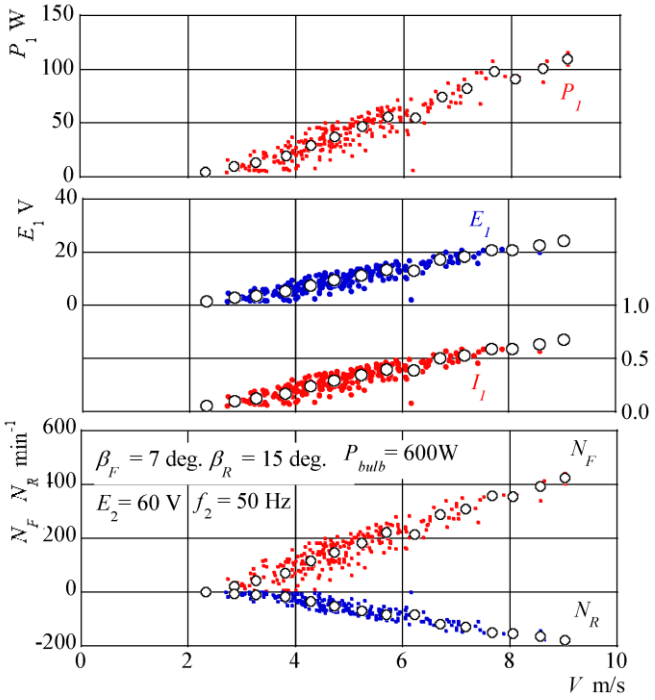

Fig. 7 Example of the performance at the natural wind

Figure 8 shows just a small sample for how to adjust the exciting voltage E_2, the exciting frequency f_2 and the blade setting angle of the rear wind rotor β_R, to keep the active output P_1 constant at the rated operation, while the induced voltage E_1 = 50 V and the induced frequency f_1 = 60 Hz. The output and the power quality can be guaranteed well with the reasonable adjustments of E_2 and f_2 at the secondary circuit and β_R. The wind power station can provide the net output P_N for the grid system, where $P_N = P_1$ - square-root (3)E_2I_2 *where* I_2 is the electric current in the secondary circuit.

The rotational direction of the rear wind rotor does not change from the counter-rotation, at the comparatively slower wind velocity in Figs. 7 and 8.

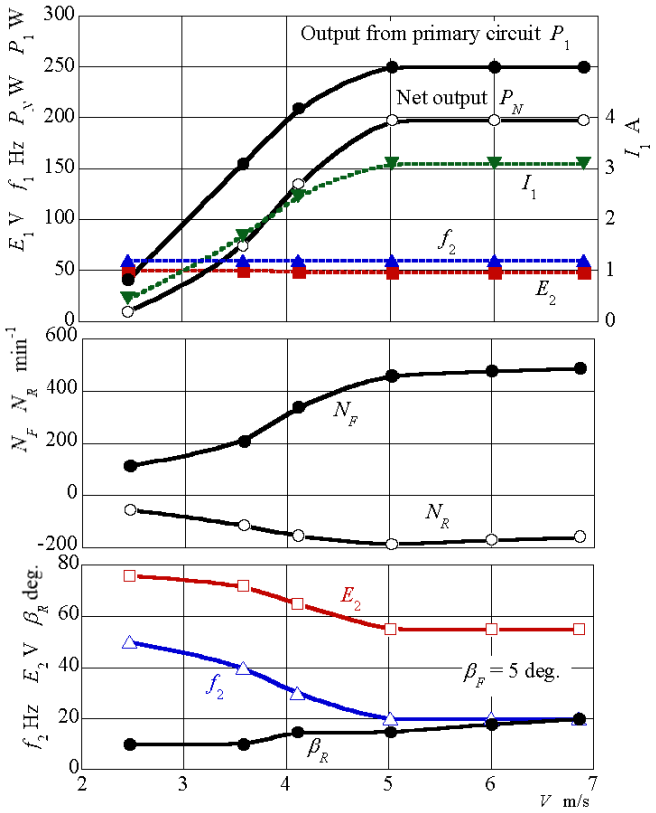

Fig. 8 Guarantee of the output and the power quality

IV. Concludig Remarks

The blade setting angle of the rear wind rotor was adjusted, not only to get a maximum efficiency at lower wind velocity but also to keep the output constant at the rated operation in the laboratory experiments. The model unit with the double rotational armature type doubly-fed induction generator was also exposed in the natural wind circumstance. The output and the power quality from the primary circuit can be guaranteed well with the adjustment of the exciting voltage and frequency at the secondary circuit and the blade setting angle of the rear wind rotor.

References

[1] T. Kanemoto, Ahmed Mohamed Galal, Y. Inada and Y. Konno, "Intelligent Wind Turbine Generator with Tandem Rotors Applicable to Offshore Wind Farm", *Proceedings of the 15th International Offshore and Polar Engineering Conference and Exhibition*, 1, Seoul, Korea, pp.457-462, 2005.

[2] T. Kanemoto and Ahmed Mohamed Galal, "Development of Intelligent Wind Turbine Generator with Tandem Wind Rotors and Double Rotational Armatures (1st Report, Superior Operation of Tandem Wind Rotors)", *JSME International Journal*, Series B, 49, No.2, pp.363-368, 2006.

[3] A. Sper. David, "Wind Turbine Technology", *ASME Press*: New York, p. 93, 1994.
[4] http://www.kowintec.com/English/intro/info.htm
[5] I. Ushiyama, T. Shimota and Y Miura, "An Experimental Study of the Two Staged Wind Turbines," *Proceedings of World Renewable Energy Conference*; 909-912, 1996.
[6] T. J. Jang & H. K. Heo, "Study on the development of wind power system using mutually opposite rotation of dual rotors", *Proc. of the Renewable Energy 2008*, CD-ROM O-WE-015, 2008.
[7] K. Appa, "Counter rotating wind turbine system" *Energy Innovations Small Grant (EISG) Program Technical Report*, 2002.
[8] S. N. Jung, T. S. No & K. W. Ryu, "Aerodynamic Performance prediction of 30kW counter-rotating wind turbine system" *Renewable Energy*, Vol. 30, No. 5, pp. 631-644, 2005.
[9] W. Z. Shen, V. A. K. Zakkam, J. N. Sørensen & K. Appa, "Analysis of Counter-Rotating Wind Turbines", *Journal of Physics*: *Conference Series*, 75 012003(9pp), 2007.
[10] K. Kubo and T. Kanemoto, "Performances and Acoustic Noise of Intelligent Wind Power Unit", R*enewable Energy & Power Quality Journal*, No.9, 445, 2011.
[11] Edited by T. Wei, "Wind Power Generation and Wind Turbine D esign", *WIT Press*, pp. 333-360, 2010.
[12] Y. Usui, K. Kubo, and T. Kanemoto, "Intelligent Wind Power Unit with Tandem Wind Rotors and Double Rotational Armatures (Optimization of Blade Profiles in Front Wind Rotor)", *Journal of Energy and Power Engineering*, Vol. 6, No. 11, pp.1791-1799, 2012.
[13] K. Kubo and T. Kanemoto, "Development of Intelligent Wind Turbine Unit with Tandem Wind Rotors and Double Rotational Armatures (2nd Report, Characteristics of tandem wind rotors)", *JSME International Journal*, Ser. B, Vol. 3, No. 3, pp. 370-378, 2008.
[14] Performance and geometry of airfoil supply system, online at: http://riodb.ibase.aist.go.jp/db060/index.html
[15] R.E. Sheldahl, P.C. Klimas, Aerodynamic characteristics of seven symmetrical airfoil sections through 180-degree angle of attack for use in aerodynamic analysis of vertical axis wind turbines, *Technical report of Sandia National Laboratory*, 27-40, 1981.
[16] T. Kanemoto, Ahmed Mohamed Galal, K. Ikeda, H. Mitarai, and K. Kubo, "Intelligent Wind Turbine Generator with Tandem Rotors Applicable to Offshore Wind Farm (Characteristics of Peculiar Generator, and Performance of Three Dimensional Blades)", *Proceedings of the 17th International Offshore and Polar Engineering Conference*, Lisbon, Portugal, pp.363-368, 2007.
[17] IEC 61400-12-1: Power Performance Measurements of Electricity Producing Wind Turbines.